

# Investigation of deep levels in *n*-type 4H-SiC epilayers irradiated with low-energy electrons

Katsunori Danno and Tsunenobu Kimoto

*Department of Electronic Science and Engineering, Kyoto University, Kyotodaigaku-katsura, Nishikyo, Kyoto 615-8510, Japan*

(Received 7 August 2006; accepted 3 October 2006; published online 14 December 2006)

Deep levels in *n*-type 4H-SiC epilayers have been investigated by deep level transient spectroscopy (DLTS). The  $Z_{1/2}$  and  $EH_{6/7}$  centers are dominant in as-grown samples. After electron irradiation at 116 keV, by which only carbon atoms may be displaced, the  $Z_{1/2}$  and  $EH_{6/7}$  concentrations are significantly increased. The  $Z_{1/2}$  and  $EH_{6/7}$  centers are stable up to 1500–1600 °C and their concentrations are decreased by annealing at 1600–1700 °C. In the irradiated samples, the trap concentrations of the  $Z_{1/2}$  and  $EH_{6/7}$  centers are increased with the 0.7 power of the electron fluence. The concentrations of the  $Z_{1/2}$  and  $EH_{6/7}$  centers are very close to each other in all kinds of samples, as-grown, as-irradiated, and annealed ones, even though the condition of growth, irradiation (energy and fluence), and annealing has been changed. This result suggests that both  $Z_{1/2}$  and  $EH_{6/7}$  centers microscopically contain the same defect such as a carbon vacancy. © 2006 American Institute of Physics. [DOI: 10.1063/1.2401658]

## I. INTRODUCTION

Silicon carbide (SiC) is an attractive material for realizing high-power, high-temperature, and high-frequency devices, owing to its superior properties such as wide band gap, high breakdown field, high thermal conductivity, and high saturation electron drift velocity.<sup>1</sup> 4H-SiC has been regarded as the most promising polytype for vertical-type high-voltage devices, due to higher bulk mobility and smaller anisotropy. High-voltage (300–1200 V) 4H-SiC Schottky barrier diodes are now on the market. In addition, several field-effect transistors (FETs) such as metal-oxide-semiconductor FETs will be released in a next few years, although some problems should be overcome. To realize SiC power devices with much higher blocking voltage (more than several kilovolts), however, bipolar devices such as pin diodes, thyristors, and insulated gate bipolar transistors are more attractive in terms of lower on-resistance owing to the effect of conductivity modulation.<sup>2,3</sup>

Deep levels act as recombination and generation centers in such devices. The concentration of deep levels should be decreased because long lifetime is essential to obtain sufficient conductivity modulation. Too long a lifetime, on the other hand, will lead to considerably large switching loss in the devices mentioned above. Therefore, the concentrations of deep levels must be controlled to achieve an optimum lifetime value and its profile. Electron irradiation is one of the promising methods to control the concentrations of deep levels in silicon.<sup>4,5</sup> Defects in electron-irradiated 4H-SiC have been studied by several groups<sup>6–8</sup> using deep level transient spectroscopy (DLTS).<sup>9</sup> Hemmingsson *et al.* made 2.5 MeV electron irradiation with a fluence ranging from  $5 \times 10^{13}$  to  $10^{15}$  cm<sup>-2</sup> onto 4H-SiC epilayers.<sup>6</sup> By DLTS on the irradiated epilayers, they detected seven electron traps ( $EH_1$ ,  $EH_2$ ,  $EH_3$ ,  $EH_4$ ,  $EH_5$ ,  $EH_{6/7}$ ) and one hole trap ( $HH_1$ ). Storasta *et al.* performed low-energy electron irradiation at 80–300 keV onto 4H-SiC epilayers and investigated deep

levels induced by the low-energy electron irradiation.<sup>8</sup> By the electron irradiation at 160 keV, which may introduce only the carbon displacement,<sup>10</sup> they found the linear increase of the  $Z_{1/2}$  (see Ref. 11) and  $EH_{6/7}$  centers with increasing irradiation time. They suggested the  $Z_{1/2}$  and  $EH_{6/7}$  centers may be related to carbon displacement.

In these studies, the dependence of the trap concentrations on electron energy and electron fluence, and their thermal stability in irradiated samples, which are required for control of deep levels, have not always been presented.

In this work, the authors have investigated impacts of electron irradiation on deep levels in *n*-type 4H-SiC epilayers by DLTS. The authors also discuss the origins of deep levels induced by low-energy (80–400 keV) electron irradiation.

## II. EXPERIMENTAL PROCEDURE

Samples used in this study were *n*-type 4H-SiC(0001) epilayers grown by horizontal hot-wall chemical vapor deposition (CVD) in the authors' group.<sup>12</sup> The net donor concentration of the samples determined by capacitance-voltage (*C-V*) measurements was in the range from  $8.0 \times 10^{14}$  to  $1.6 \times 10^{16}$  cm<sup>-3</sup>, and the thickness was 10–15 μm. Nickel was thermally evaporated onto the sample surface as Schottky contacts with a thickness of approximately 70 nm. The typical diameter of the Schottky contacts was 1500 μm. Ohmic contacts were formed with silver paste on the backside of highly doped *n*-type substrates.

Deep levels in as-grown and irradiated 4H-SiC were investigated by DLTS in the temperature range from 100 to 700 K. If not specified, the reverse bias was kept at -5 V, and the pulse voltage applied during the DLTS measurements was 0 V (pulse height: 5 V). A period width of 0.2 s was employed for all the DLTS measurements performed in this study. A Fourier transform analysis<sup>13</sup> of the measured transients was employed. Temperature-independent capture

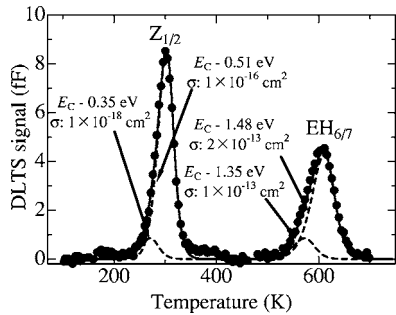


FIG. 1. DLTS spectrum of as-grown *n*-type 4H-SiC epilayer (closed circles). Fit for the spectrum is also shown (broken line: fit for each trap, solid line: sum of the each fit).

cross section was assumed when analyzing the DLTS data. In this article, the trap concentrations are corrected by considering the lambda effect.<sup>14</sup> Near the Ni/SiC Schottky interface, there is the region, where a deep level is energetically located above the Fermi level when the filling pulse voltage is applied, even though the deep level is located below the Fermi level in the most part of the depletion layer. In this near-surface region, electrons are not captured by the traps during the filling pulse. Near the opposite edge of a depletion layer, a deep level is located below the Fermi level even when the reverse bias is applied. In this region, electrons are always trapped by deep levels and are not emitted. Due to these effects, the trap concentration without the correction is underestimated.

After identification of deep levels in as-grown epilayers by DLTS, the authors performed the low-energy electron irradiation at an energy of 80–400 keV and with a fluence of  $3 \times 10^{15}$ – $3 \times 10^{18}$  cm<sup>-2</sup>. By irradiation at lower than 200 keV, displacement of carbon atoms mainly takes place<sup>10</sup> and at the energy higher than 200 keV, displacement of both carbon and silicon atoms is introduced. All the irradiation was performed in atmospheric nitrogen ambient without intentional heating.

### III. RESULTS

#### A. DLTS of as-grown *n*-type 4H-SiC

Figure 1 shows the DLTS spectrum of an as-grown *n*-type 4H-SiC epilayer (nitrogen-doped, net donor concentration ( $N_d$ ):  $4.1 \times 10^{15}$  cm<sup>-3</sup>) in the temperature range from 100 to 700 K. The DLTS spectrum was dominated by two peaks. These DLTS peaks can be assigned to the  $Z_{1/2}$  ( $E_C - 0.56$  eV) (see Ref. 11) and  $EH_{6/7}$  ( $E_C - 1.45$  eV) (see Ref. 6) centers from the Arrhenius plot of emission time constant assuming temperature-independent capture cross section (not shown). Their concentrations were  $5.8 \times 10^{12}$  cm<sup>-3</sup> for the  $Z_{1/2}$  center and  $3.8 \times 10^{12}$  cm<sup>-3</sup> for the  $EH_{6/7}$  center in this particular sample. The  $Z_{1/2}$  and  $EH_{6/7}$  peaks are rather asymmetric, and show a “tail” in their lower temperature range. Since this may be explained by overlapping of several peaks, fitting the spectrum was tried to investigate these peaks. In Fourier transform DLTS, the spectrum for one deep trap is given by<sup>13</sup>

$$b_1 = \frac{N_T C_{st}}{T_W N_d} \left[ \exp\left(-\frac{T_W}{\tau}\right) - 1 \right] \frac{2\pi/T_W}{1/\tau^2 + (2\pi/T_W)^2}, \quad (1)$$

where  $b_1$  is the DLTS signal,  $N_T$  the trap concentration,  $C_{st}$  the capacitance under the reverse bias condition,  $T_W$  the period width, and  $\tau$  the emission time constant. The emission time constant is given by

$$\tau = \frac{1}{N_C \sigma v_{th}} \exp\left(\frac{E_C - E_T}{kT}\right), \quad (2)$$

where  $N_C$  is the effective density of states in the conduction band,  $\sigma$  the capture cross section,  $v_{th}$  thermal velocity,  $E_C$  the energy level of the conduction band edge,  $E_T$  the energy level of the trap, and  $k$  the Boltzmann constant. The authors used  $\sigma$  and  $E_C - E_T$  as the parameters for the fit. The fit of Eq. (1) to the experimental data results in four DLTS peaks (broken line), and the sum of the individual curves is presented as the solid curve, while the spectrum experimentally obtained is plotted by closed circles. The energy levels and capture cross sections, which give the best fit, for four deep levels are shown in Fig. 1.

The peak of the  $EH_{6/7}$  center is composed of the two traps. From the fitting, their activation energies were estimated to be 1.35 eV ( $EH_6$ ) and 1.48 eV ( $EH_7$ ). The concentration of the  $EH_7$  center ( $N_T$ :  $3.7 \times 10^{12}$  cm<sup>-3</sup>) was much higher than that of the  $EH_6$  center ( $N_T$ :  $7.3 \times 10^{11}$  cm<sup>-3</sup>). The peak at 290 K is also composed of two peaks. The peak is the overlapping of an unknown trap (detected at lower temperature) and the  $Z_{1/2}$  center (detected at higher temperature). Note that the  $Z_1$  and  $Z_2$  centers cannot be observed separately under the present measurement condition without light illumination.<sup>15</sup> The concentration of the  $Z_{1/2}$  center was  $5.8 \times 10^{12}$  cm<sup>-3</sup>, which is one order of magnitude higher than that of the unknown trap ( $5.7 \times 10^{11}$  cm<sup>-3</sup>). The actual concentration of the  $Z_{1/2}$  center is half of the value described in this article due to the negative- $U$  nature.<sup>15,16</sup>

#### B. DLTS of electron-irradiated *n*-type 4H-SiC

In the first series of irradiation experiments, the electron irradiation was performed onto *n*-type samples at energy of 116 keV in the fluence range from  $3 \times 10^{15}$  to  $3 \times 10^{18}$  cm<sup>-2</sup>. Figure 2(a) shows the DLTS spectra of the as-grown sample (same as that in Fig. 1), the sample irradiated with a fluence of  $3 \times 10^{17}$  cm<sup>-2</sup>, and the irradiated sample annealed at 950 °C for 30 min in atmospheric Ar ambient. As shown in Fig. 2(a), the trap concentrations were significantly increased to  $7.6 \times 10^{13}$  cm<sup>-3</sup> for the  $Z_{1/2}$  center (neglecting the unknown trap at  $E_C - 0.35$  eV) and to  $7.4 \times 10^{13}$  cm<sup>-3</sup> for the  $EH_{6/7}$  center by the irradiation. This result indicates that both the  $Z_{1/2}$  and  $EH_{6/7}$  centers are related to carbon displacement since carbon displacement is mainly introduced by the electron irradiation at 116 keV.<sup>8,10</sup> The net donor concentration determined by  $C$ - $V$  measurements was kept constant regardless of the electron irradiation.

In the as-irradiated sample, several peaks were newly observed at 125 K (indicated by ET1), at 350 K (ET2, shoulder of the  $Z_{1/2}$  center) and 470 K (ET3). They may be also related to carbon displacement. The concentration and en-

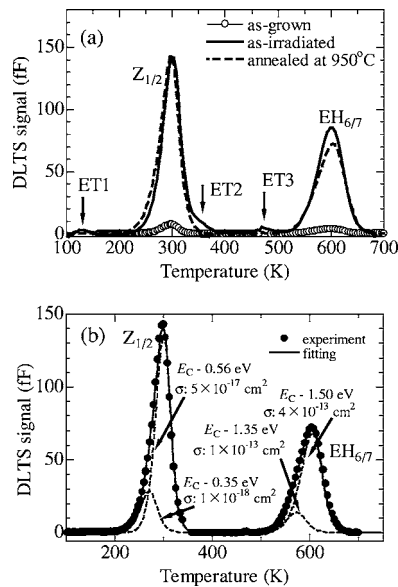


FIG. 2. (a) DLTS spectra of as-grown, as-irradiated, and annealed 4H-SiC epilayers. Samples were irradiated at an energy of 116 keV with a fluence of  $3 \times 10^{17} \text{ cm}^{-2}$ . Thermal annealing following the irradiation was performed at  $950^\circ \text{C}$  for 30 min. (b) Fit for the spectrum taken from the annealed epilayer is also shown (broken line: fit for each trap, solid line: sum of the each fit).

ergy level of the trap detected at 125K (ET1) are  $1.5 \times 10^{12} \text{ cm}^{-3}$  and  $E_C - 0.16 \text{ eV}$ , respectively. The energy level of this trap is very close to that of  $P_1/P_2$ ,  $ID_1$  or  $ID_2$  centers,<sup>11</sup> which were detected after  $\text{He}^+$  ( $P_1/P_2$ ) or  $\text{Ti}^+$  (or  $\text{V}^+$ ) implantation ( $ID_1$  or  $ID_2$ ) and subsequent annealing at more than  $1000^\circ \text{C}$ . On the other hand, the trap ET1 was thermally unstable, and the concentration was decreased below the detection limit (approximately  $1 \times 10^{11} \text{ cm}^{-3}$ ) after the DLTS measurement up to 700 K. Therefore, this unknown trap (ET1) may be different from  $P_1/P_2$ ,  $ID_1$ , and  $ID_2$  centers. The unknown trap (ET2) may be same as the  $\text{EH}_3$  center,<sup>6</sup> according to the DLTS peak temperature. The concentration and activation energy of the trap detected at 470 K (ET3) were  $3.9 \times 10^{12} \text{ cm}^{-3}$  and about 1 eV, respectively. This trap could be observed after DLTS measurement up to 700 K, but was decreased in concentration below the detection limit after the annealing at  $950^\circ \text{C}$ . According to the energy level and thermal stability, the trap ET3 may be the same trap as the  $\text{RD}_3$  center,<sup>11</sup> which was detected after  $\text{He}^+$  implantation and subsequent annealing at  $430^\circ \text{C}$ .

In the annealed sample, the ET1, ET2, and ET3 peaks disappeared, while the  $Z_{1/2}$  and  $\text{EH}_{6/7}$  centers were two dominant traps in the temperature range from 100 to 700 K. Both the centers showed no meaningful change in their concentrations after annealing at  $950^\circ \text{C}$ .

In Fig. 2(b), the authors made fitting the DLTS spectrum for the sample irradiated with a fluence of  $3 \times 10^{17} \text{ cm}^{-2}$  and annealed at  $950^\circ \text{C}$ . The DLTS spectrum can be again fitted by considering four traps, as in Fig. 1. As shown in the Fig. 2(b), the trap concentrations were increased to  $1.3 \times 10^{13} \text{ cm}^{-3}$  for the  $\text{EH}_6$  center and  $6.5 \times 10^{13} \text{ cm}^{-3}$  for the  $\text{EH}_7$  center. Note that the ratio between  $\text{EH}_6$  and  $\text{EH}_7$  concentrations was kept almost constant, i.e., 1/5, both in as-grown and irradiated samples. The origins of the  $Z_{1/2}$  and  $\text{EH}_{6/7}$  centers are discussed in the next section.

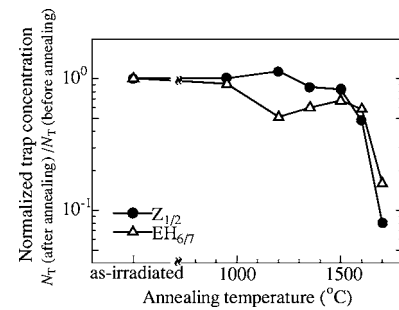


FIG. 3. Annealing temperature dependence of normalized trap concentrations [ $N_T$  (after annealing)/ $N_T$  (before annealing)] for the  $Z_{1/2}$  and  $\text{EH}_{6/7}$  centers in 4H-SiC. Electron irradiation was performed at 116 keV with a fluence of  $9 \times 10^{17} \text{ cm}^{-2}$ . Trap concentrations of as-irradiated samples were  $(1-2) \times 10^{14} \text{ cm}^{-3}$  for both the  $Z_{1/2}$  and  $\text{EH}_{6/7}$  centers.

Figure 3 shows the annealing temperature dependence of normalized  $Z_{1/2}$  and  $\text{EH}_{6/7}$  concentrations (trap concentrations after annealing divided by the concentration before annealing). The samples were irradiated at 116 keV with a fluence of  $9 \times 10^{17} \text{ cm}^{-2}$ . In the as-irradiated samples, the trap concentrations were  $(1.1-1.6) \times 10^{14} \text{ cm}^{-3}$  for the  $Z_{1/2}$  center and  $(0.89-1.7) \times 10^{14} \text{ cm}^{-3}$  for the  $\text{EH}_{6/7}$  center. Thermal annealing was performed at  $950-1700^\circ \text{C}$  for 30 min in atmospheric Ar ambient. As shown in Fig. 3, both the traps were stable up to  $1500-1600^\circ \text{C}$ . Their concentrations were, however, decreased by annealing at  $1600-1700^\circ \text{C}$ , and the concentrations were reduced to  $8.0 \times 10^{12} \text{ cm}^{-3}$  ( $Z_{1/2}$ ) and  $6.7 \times 10^{12} \text{ cm}^{-3}$  ( $\text{EH}_{6/7}$ ) by annealing at  $1700^\circ \text{C}$ . This annealing stage is very similar to that in the as-grown samples.<sup>17</sup> The similar thermal stability was reported in epilayers irradiated with 15-MeV electrons.<sup>18</sup> During these annealing experiments (and DLTS measurements), no new DLTS peaks were observed in the temperature range of 100–700 K.

Figure 4 shows the dependence of increase in the  $Z_{1/2}$  and  $\text{EH}_{6/7}$  concentrations by the 116 keV irradiation ( $\Delta N_T$ ) on the electron fluence.  $\Delta N_T$  for the  $Z_{1/2}$  and  $\text{EH}_{6/7}$  centers in the irradiated samples increased by increasing the electron fluence in the wide range over three orders of magnitude. The  $\Delta N_T$  is in proportional to the 0.7 power of the fluence for both centers. In the ideal case, the concentration would increase with a slope of unity if the center originates from a simple isolated defect like a single carbon vacancy. In the present results, the slope of the plot (0.7) is smaller than the

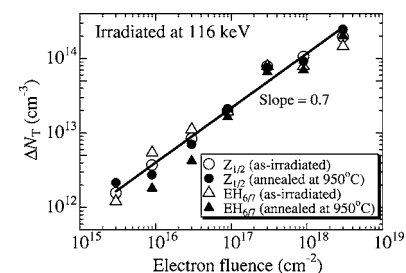


FIG. 4. Dependence of increase in  $Z_{1/2}$  and  $\text{EH}_{6/7}$  concentrations by electron irradiation ( $\Delta N_T$ ) on the electron fluence (energy: 116 keV). Open symbols represent the concentration for as-irradiated samples and closed symbols for  $950^\circ \text{C}$ -annealed samples. The solid line is a least-squares fitting for both traps in as-irradiated samples.

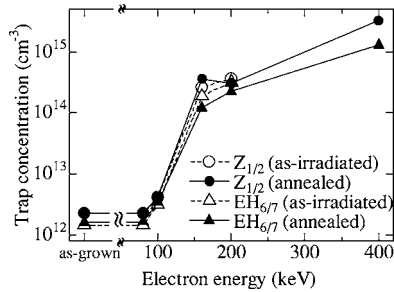


FIG. 5. Dependence of the  $Z_{1/2}$  and  $EH_{6/7}$  concentrations in both as-irradiated and annealed (950 °C for 30 min) samples on the irradiation energy. The irradiation condition is changed by maintaining the product of the electron energy and fluence at  $1.6 \times 10^{19}$  keV/cm<sup>2</sup>.

ideal case. The possible reasons are: (1) increase of the sample temperature during the irradiation and/or (2) complex origins of the centers. The irradiation was performed for more than ten hours when the fluence was  $3 \times 10^{18}$  cm<sup>-2</sup>. The temperature of sample surface may be increased with the irradiation time (electron fluence) although the samples were placed on a water-cooled plate during the irradiation. Since unintentional heating in the irradiated region can suppress the formation of point defects,  $\Delta N_T$  might tend to saturate in the samples irradiated at high fluence. Therefore the first reason (unintentional heating) may be a dominant factor to reduce the slope in Fig. 4. If the  $Z_{1/2}$  and  $EH_{6/7}$  centers are complexes, their concentrations will not be increased in the as-irradiated samples. This is because a complex will not be formed without annealing. If the formation energy of a complex is very low, however, a complex can be formed by the unintentional heating. In such a case, the second reason may affect the slope of the plot.

Figure 5 shows the dependence of the  $Z_{1/2}$  and  $EH_{6/7}$  concentrations on the electron energy in both as-irradiated and annealed (950 °C for 30 min) samples. The irradiation condition was changed by maintaining the product of the electron energy and fluence at  $1.6 \times 10^{19}$  keV/cm<sup>2</sup>. For the sample irradiated at 80 keV, no increase was found in both the  $Z_{1/2}$  and  $EH_{6/7}$  concentrations. As shown in the figure, the concentrations of the both traps started to increase by the irradiation at 100 keV and continued to increase by increasing the electron energy in the as-irradiated and 950 °C-annealed samples. In the sample irradiated with 400-keV electrons, the reliable DLTS spectra could not be obtained without annealing, since the generated deep levels completely compensated the donors. From the results, carbon displacement will be introduced by the irradiation at the energy higher than 80–100 keV. The displacement energy ( $E_D$ ) amounts to

$$E_D = \frac{4M_e M_a}{(M_e + M_a)^2} E_e, \quad (3)$$

where  $M_e$  is the mass of accelerated electrons,  $M_a$  the mass of C (or Si) atoms, and  $E_e$  the energy of accelerated electrons.<sup>19</sup> Substituting 80–100 keV to  $E_e$  of the equation, the displacement energy is calculated as 17–22 eV. Using this energy value, the irradiation energy required for Si displacement is obtained as 165–200 keV. Sullivan *et al.* esti-

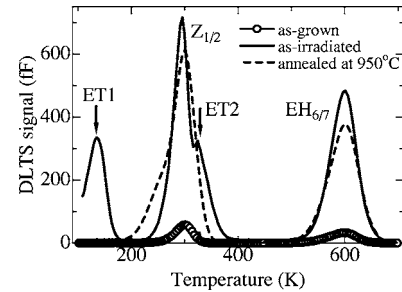


FIG. 6. DLTS spectra of samples before (open circles) and after irradiation at 200 keV with a fluence of  $8 \times 10^{16}$  cm<sup>-2</sup> (solid line: as-irradiated, broken line: annealed at 950 °C).

mated the threshold energy for Si displacement as 250 keV from the investigation on Si vacancy-related defects in electron-irradiated 4H-SiC by photoluminescence.<sup>20</sup> Their estimation for the threshold energy of Si displacement (250 keV) is larger than the present study (165–200 keV).

DLTS spectra of the samples before and after irradiation at 200 keV (fluence:  $8 \times 10^{16}$  cm<sup>-2</sup>) are shown in Fig. 6. The trap concentrations of the particular as-grown sample were  $2.7 \times 10^{13}$  cm<sup>-3</sup> for the  $Z_{1/2}$  center and  $2.2 \times 10^{13}$  cm<sup>-3</sup> for the  $EH_{6/7}$  center. By the electron irradiation, the trap concentrations were significantly increased ( $Z_{1/2}$ :  $3.7 \times 10^{14}$  cm<sup>-3</sup>,  $EH_{6/7}$ :  $3.3 \times 10^{14}$  cm<sup>-3</sup>), and two other peaks were observed at 135 and 325 K. The peak at 135 K is the same as the unknown peak observed in the sample irradiated at 116 keV [ET1 in Fig. 2(a)]. The peak at 325 K was also observed in Fig. 2(a) as the shoulder of the  $Z_{1/2}$  center, as indicated by ET2 in Fig. 2(a). Therefore these defect centers are not related to the silicon displacement. After annealing at 950 °C for 30 min, the peaks at 135 and 325 K disappeared. By 200–400 keV irradiation, no other DLTS peaks were observed in this temperature range (100–700 K), while the irradiation energies (200–400 keV) employed in this investigation are large enough to induce silicon displacement.<sup>10</sup> This result indicates that electrically active defect centers relating to silicon displacement are not introduced in the upper half of the band gap by electron irradiation under the present conditions.

#### IV. DISCUSSION

By the electron irradiation at 100–160 keV, carbon vacancies ( $V_C$ ) and carbon interstitials ( $C_i$ ) can be introduced in as-irradiated SiC samples. By annealing, they may transform into complexes such as  $V_C + \alpha$  [ $\alpha$ : point defect(s)],  $C_i + \alpha$ , and carbon anti-site ( $C_{Si}$ ).

In the present study, the  $Z_{1/2}$  and  $EH_{6/7}$  concentrations are increased in samples irradiated at 100–160 keV with or without subsequent annealing, in agreement with a previous report.<sup>8</sup> Therefore, the  $Z_{1/2}$  and  $EH_{6/7}$  centers are probably derived from single  $V_C$  or  $C_i$ . The annealing experiments reveal that the  $Z_{1/2}$  and  $EH_{6/7}$  centers are thermally stable up to 1600 °C both in as-grown<sup>17</sup> and irradiated (Fig. 3) samples. Since  $C_i$  may be thermally unstable due to its high mobility,<sup>21,22</sup> the  $Z_{1/2}$  and  $EH_{6/7}$  centers may not be  $C_i$ -related defects. Therefore, a single  $V_C$  may be a probable candidate as the origin of the  $Z_{1/2}$  and  $EH_{6/7}$  centers. On the

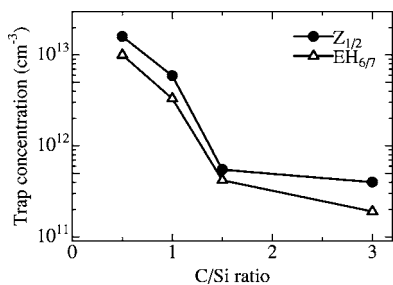


FIG. 7. Dependence of  $Z_{1/2}$  and  $EH_{6/7}$  concentrations in as-grown 4H-SiC epilayers on C/Si ratio during CVD. The epilayers were grown by horizontal hot-wall CVD at 1500 °C in a  $SiH_4-C_3H_8-H_2$  system.

other hand, thermally unstable traps such as the ET1, ET2, and ET3 centers, which are detected in as-irradiated samples and which disappeared by annealing at 950 °C, may be related to  $C_i$ . This speculation that the  $Z_{1/2}$  and  $EH_{6/7}$  centers are related not to  $C_i$  but to  $V_C$ , is supported by the fact that the  $Z_{1/2}$  and  $EH_{6/7}$  concentrations in as-grown epilayers can be reduced under C-rich condition during CVD growth,<sup>23-25</sup> although some different results are also reported.<sup>26</sup> Figure 7 shows the dependence of the  $Z_{1/2}$  and  $EH_{6/7}$  concentrations in as-grown 4H-SiC epilayers on the C/Si ratio (the ratio between C and Si atoms in supplied source gases) during CVD growth. DLTS results used in Fig. 7 were obtained from nitrogen-doped 4H-SiC epilayers grown by horizontal hot-wall CVD at 1500 °C in a  $SiH_4-C_3H_8-H_2$  system. The C/Si ratio was varied by changing the  $C_3H_8$  flow rate with a constant  $SiH_4$  flow rate of 1.5 sccm. The details of growth condition are described in Ref. 24. As shown in Fig. 7, it is obvious that the generation of  $Z_{1/2}$  and  $EH_{6/7}$  is suppressed under a high C/Si ratio (C-rich condition). This CVD result suggests that the  $Z_{1/2}$  and  $EH_{6/7}$  centers are not  $C_i$ -related but  $V_C$ -related defects,<sup>24,25</sup> because the C-rich condition is favorable to suppress  $V_C$  formation and to enhance  $C_i$  formation.

It should be noted that the  $Z_{1/2}$  and  $EH_{6/7}$  concentrations are always very close to each other when the C/Si ratio (Fig. 7), the electron fluence (Fig. 4), and the irradiation energy (Fig. 5) are changed. In the case of a divacancy ( $V_2$ ) in Si, for example, the  $(-2-)$  level at  $E_C-0.23$  eV and the  $(0/-)$  level at  $E_C-0.42$ eV could be detected by DLTS with similar concentrations if the crystal does not have large strain.<sup>27</sup> In Fig. 8, the relation between the  $Z_{1/2}$  and  $EH_{6/7}$

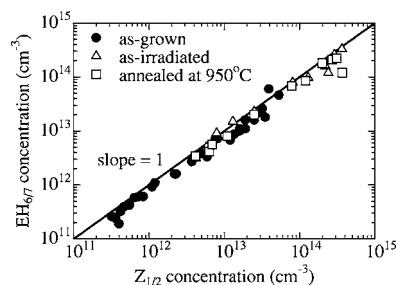


FIG. 8. The relation between the  $Z_{1/2}$  and  $EH_{6/7}$  concentrations obtained for as-grown samples, as-irradiated samples (irradiated at 100–400 keV), and irradiated samples annealed at 950 °C for 30 min.

concentrations is presented. As shown in Fig. 8, a close to one-to-one correlation was obtained for the  $Z_{1/2}$  and  $EH_{6/7}$  concentrations as observed for the  $(-2-)$  and  $(0/-)$  levels of  $V_2$  in Si. Although a slight difference in the  $Z_{1/2}$  and  $EH_{6/7}$  concentrations was observed in some samples, this is probably because the obtained concentrations may be influenced by overlapping of DLTS signals with other unknown peaks detected in the same temperature region. Furthermore, the  $Z_{1/2}$  and  $EH_{6/7}$  centers showed similar annealing stage in both as-grown<sup>17</sup> and irradiated (Fig. 3) samples. Therefore, the  $Z_{1/2}$  and  $EH_{6/7}$  centers may be attributed to the same origin but different charge states.

A single  $V_C$  is a probable candidate for the origin of the  $Z_{1/2}$  and  $EH_{6/7}$  centers according to the present results (Figs. 4, 5, and 7). Figure 9 summarizes the energy levels of the  $Z_{1/2}$  ( $E_C-0.65$  eV) and  $EH_{6/7}$  ( $E_C-1.55$  eV) centers obtained by DLTS and  $V_C$  levels calculated by first-principles calculations<sup>28,29</sup> and the levels obtained by photo electron paramagnetic resonance (EPR).<sup>30,31</sup> According to the first-principles calculations by Zywiez *et al.*,  $V_C$  forms two negative- $U$  centers at  $E_V+(1.37/1.68)$  eV and  $E_V+(2.45/2.74)$  eV for the cubic site, and  $E_V+(1.44/1.68)$  eV and  $E_V+(2.42/2.71)$  eV for the hexagonal site as shown in Fig. 9. Torpo *et al.* applied the Madelung correction to their calculation.<sup>29</sup> In their calculation,  $V_C$  does not show negative- $U$  behavior and is located at  $E_V+(0.97/1.18)$  eV for  $(2+/+)$  level,  $E_V+(1.22/1.34)$  eV for  $(+0/0)$ ,  $E_V+(2.09/2.28)$  eV for  $(0/-)$ , and  $E_V+(2.21/2.41)$  eV for  $(-2-)$ . As shown in Fig. 9, the energy levels of single  $V_C$ , calculated by Zywiez *et al.* are located relatively close to

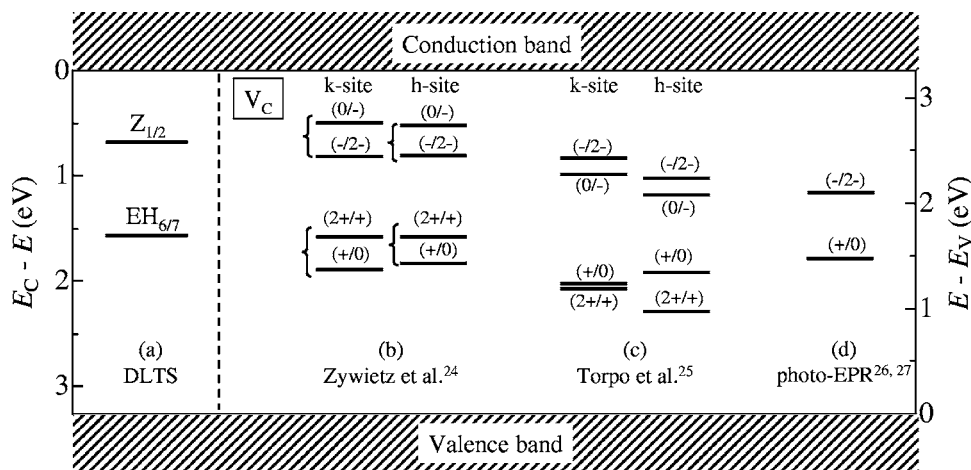


FIG. 9. Overview of ground states of (a) deep levels detected in  $n$ -type 4H-SiC epilayers by DLTS,  $V_C$  levels calculated by (b) Zywiez *et al.* (see Ref. 28) and (c) Torpo *et al.* (see Ref. 29), and  $V_C$  levels obtained by (d) photo-EPR (see Refs. 30 and 31).

those of the  $\text{EH}_{6/7}$  ( $E_V+1.71$  eV) and  $Z_{1/2}$  ( $E_V+2.61$  eV) centers. The calculated energy levels are not always accurate especially for the levels with multiple charge ( $2+$ ,  $2-$ ) due to the difficulty in calculation. Therefore, it is not easy to predict perfectly where the levels are energetically located and whether they show negative- $U$  features or not. Moreover, the energy levels might be slightly underestimated in the present DLTS results because a temperature-independent capture cross section was assumed. Therefore, it is important here that the DLTS results do not show significant conflict with theoretical predictions, though some quantitative discrepancy is observed between experimental and theoretical levels.

Son *et al.*<sup>30</sup> revealed that the donor ( $+/0$ ) level of  $V_C$  is energetically located at  $E_V+1.47$  eV by photo-EPR on electron-irradiated  $p$ -type 4H-SiC. Using photo-EPR on  $n$ -type 4H-SiC, Umeda *et al.* suggested that the double acceptor ( $-/2-$ ) level of  $V_C$  is located at  $E_C-1.08$  eV. As shown in Fig. 9, the  $V_C$  levels detected by photo EPR do not conflict with those of the  $Z_{1/2}$  and  $\text{EH}_{6/7}$  levels, because the energy levels determined by optical measurements are generally deeper than those obtained by DLTS. Therefore, the authors speculate that both the  $Z_{1/2}$  and  $\text{EH}_{6/7}$  centers may originate from single  $V_C$  (but different charge states). However, a defect complex including  $V_C$  ( $V_C+\alpha$ ) cannot still be ruled out as the origin of the  $Z_{1/2}$  and  $\text{EH}_{6/7}$  centers. This is because the complex can be formed in “as-irradiated samples” if the migration energy of defect  $\alpha$  is lower than thermal energy provided by the unintentional heating (approximately 100–200 °C) during irradiation. According to the theoretical calculations mentioned above (Fig. 9), however, at least two single  $V_C$  levels will be detected in the temperature region, scanned in our DLTS measurements. Therefore, it is reasonable to speculate that the different single  $V_C$  levels correspond to the  $Z_{1/2}$  and  $\text{EH}_{6/7}$  centers. For identification of the centers, however, more accurate calculation and further experimental investigation are required.

## V. CONCLUSIONS

The authors investigated deep levels in  $n$ -type 4H-SiC epilayers irradiated with low-energy (80–400 keV) electrons by DLTS. The  $Z_{1/2}$  and  $\text{EH}_{6/7}$  concentrations were increased by increasing the fluence of low-energy (116 keV) electrons, indicating that the centers are related to the carbon displacement, or generation of carbon vacancies and interstitials. From thermal stability and C/Si dependence during CVD of the centers, they may be  $V_C$ -related defects. The  $Z_{1/2}$  and  $\text{EH}_{6/7}$  concentrations were close to each other in all kinds of samples, as-grown, as-irradiated, and annealed ones, irrespective of the conditions of growth, irradiation, and annealing. The  $Z_{1/2}$  and  $\text{EH}_{6/7}$  centers showed almost same annealing stage and their concentrations decreased by annealing at 1600–1700 °C. Moreover, the dependence of the  $Z_{1/2}$  and  $\text{EH}_{6/7}$  concentrations on the C/Si ratio during CVD growth was also nearly identical. Therefore, the  $Z_{1/2}$  and  $\text{EH}_{6/7}$  centers may be derived from a same origin ( $V_C$ -related defect)

but different charge state. In the samples irradiated at 200-keV or 400-keV electrons, no additional DLTS peaks could be found in the temperature range from 100 to 700 K.

## ACKNOWLEDGMENTS

The authors thank Dr. H. Kaneko and Dr. O. Sakamoto at NHV Corp. for electron-irradiation experiments. This work was financially supported in part by a Grand-in-Aid for the Fundamental Research (No. 18206032) and the 21st century COE program (No. 14213201) from the Ministry of Education, Culture, Sports, Science and Technology, Japan.

- <sup>1</sup>M. Bhatnagar and B. J. Baliga, IEEE Trans. Electron Devices **40**, 645 (1993).
- <sup>2</sup>H. Lendenmann, F. Dahlquist, J. P. Bergman, H. Bleichner, and C. Hallin, Mater. Sci. Forum **389–393**, 1259 (2002).
- <sup>3</sup>Y. Sugawara, D. Takayama, K. Asano, A. Agarwal, S. Ryu, J. Palmour, and S. Ogata, Proceedings of the International Symposium on Power Semiconductor Devices & ICs 2004, Kitakyusyu, 2004, pp. 365–368.
- <sup>4</sup>B. J. Baliga and E. Sun, IEEE Trans. Electron Devices **24**, 685 (1977).
- <sup>5</sup>R. O. Carlson, Y. S. Sun, and H. B. Assalit, IEEE Trans. Electron Devices **24**, 1103 (1977).
- <sup>6</sup>C. Hemmingsson, N. T. Son, O. Kordina, J. P. Bergman, E. Janzén, J. L. Lindström, S. Savage, and N. Nordell, J. Appl. Phys. **81**, 6155 (1997).
- <sup>7</sup>G. Alfieri, E. V. Monakhov, and B. G. Svensson, Mater. Sci. Forum **457–460**, 481 (2004).
- <sup>8</sup>L. Storasta, J. P. Bergman, E. Janzén, A. Henry, and J. Lu, J. Appl. Phys. **96**, 4909 (2004).
- <sup>9</sup>D. V. Lang, J. Appl. Phys. **45**, 3023 (1974).
- <sup>10</sup>H. J. von Bardeleben, J. L. Cantin, L. Henry, and M. F. Barthe, Phys. Rev. B **62**, 10841 (2000).
- <sup>11</sup>T. Dalibor, G. Pensl, H. Matsunami, T. Kimoto, W. J. Choyke, A. Schöner, and N. Nordell, Phys. Status Solidi A **162**, 199 (1997).
- <sup>12</sup>T. Kimoto, S. Nakazawa, K. Hashimoto, and H. Matsunami, Appl. Phys. Lett. **79**, 2761 (2001).
- <sup>13</sup>S. Weiss and R. Kassing, Solid-State Electron. **31**, 1733 (1988).
- <sup>14</sup>S. D. Brotherton, Solid-State Electron. **26**, 987 (1983).
- <sup>15</sup>C. G. Hemmingsson, N. T. Son, A. Ellison, J. Zhang, and E. Janzén, Phys. Rev. B **58**, R10119 (1998).
- <sup>16</sup>G. D. Watkins and J. R. Troxell, Phys. Rev. Lett. **44**, 593 (1980).
- <sup>17</sup>Y. Negoro, T. Kimoto, and H. Matsunami, Appl. Phys. Lett. **85**, 1716 (2004).
- <sup>18</sup>G. Alfieri, E. V. Monakhov, B. G. Svensson, and M. K. Linnarsson, J. Appl. Phys. **98**, 043518 (2005).
- <sup>19</sup>H. Ryssel and I. Ruge, *Ion Implantation* (Wiley, New York, 1986).
- <sup>20</sup>W. Sullivan and J. W. Steeds, Mater. Sci. Forum **527–529**, 481 (2006).
- <sup>21</sup>M. Bockstedte, A. Mattausch, and O. Pankratov, in *Silicon Carbide, Recent Major Advances*, edited by W. J. Choyke, H. Matsunami, and G. Pensl (Springer, Berlin, 2003), pp. 27–55.
- <sup>22</sup>F. Gao, W. J. Weber, M. Posselt, and V. Belko, Mater. Sci. Forum **457–460**, 457 (2004).
- <sup>23</sup>K. Fujihira, T. Kimoto, and H. Matsunami, J. Cryst. Growth **255**, 136 (2003).
- <sup>24</sup>T. Kimoto, K. Hashimoto, and H. Matsunami, Jpn. J. Appl. Phys., Part 1 **42**, 7294 (2003).
- <sup>25</sup>C. W. Litton, D. Johnstone, S. Akarca-Biyikli, K. S. Ramaiah, I. Bhat, T. P. Chow, J. K. Kim, and E. F. Schubert, Appl. Phys. Lett. **88**, 121914 (2006).
- <sup>26</sup>I. Pintilie, L. Pintilie, and K. Imscher, Appl. Phys. Lett. **81**, 4841 (2002).
- <sup>27</sup>B. G. Svensson and M. Willander, J. Appl. Phys. **62**, 2758 (1987).
- <sup>28</sup>A. Zywiets, J. Furthmüller, and F. Bechstedt, Phys. Rev. B **59**, 15166 (1999).
- <sup>29</sup>L. Torpo, M. Marlo, T. E. M. Staab, and R. M. Nieminen, J. Phys.: Condens. Matter **13**, 6203 (2001).
- <sup>30</sup>N. T. Son, B. Magnusson, and E. Janzén, Appl. Phys. Lett. **81**, 3945 (2002).
- <sup>31</sup>T. Umeda, Y. Ishitsuka, J. Isoya, N. T. Son, E. Janzén, N. Morishima, T. Ohshima, H. Itoh, and A. Gali, Phys. Rev. B **71**, 193202 (2005).